

# Synthesis and Evaluation of Novel Cyclic Peptide Inhibitors of Lysine-Specific Demethylase 1

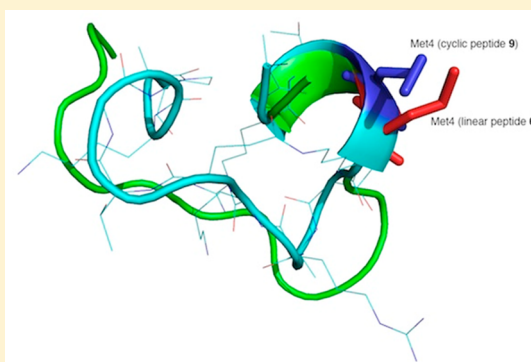
Isuru R. Kumarasinghe and Patrick M. Woster\*

Department of Drug Discovery and Biomedical Sciences, Medical University of South Carolina, 70 President Street, Charleston, South Carolina 29425, United States

## Supporting Information

**ABSTRACT:** Lysine specific demethylase 1 (LSD1) selectively removes methyl groups from mono- and dimethylated histone 3 lysine 4 (H3K4), resulting in gene silencing. LSD1 is overexpressed in many human cancers, resulting in aberrant silencing of tumor suppressor genes. Thus, LSD1 is a validated target for the discovery of antitumor agents. Using a ligand-based approach, we designed and synthesized a series of cyclic and linear peptides that are effective inhibitors of LSD1. Linear peptide 7 and cyclic peptide 9 inhibited LSD1 in vitro by 91 and 94%, respectively, at a concentration of 10  $\mu$ M. Compound 9 was a potent LSD1 inhibitor ( $IC_{50}$  2.1  $\mu$ M;  $K_i$  385 nM) and had moderate antitumor activity in the MCF-7 and Calu-6 cell lines in vitro. Importantly, 9 is significantly more stable to hydrolysis in rat plasma than the linear analogue 7. The cyclic peptides described herein represent important lead structures in the search for inhibitors of flavin-dependent histone demethylases.

**KEYWORDS:** Chromatin architecture, chromatin remodeling, lysine specific demethylase, cyclic peptide, KDM inhibitors, histone, histone 3 lysine 4



Histone proteins occur as octamers that consist of one H3–H4 tetramer and two H2A–H2B dimers.<sup>1</sup> These proteins interact with double-stranded DNA in such a way that approximately 146 base pairs are wrapped around the histone octamer to form a nucleosome. Lysine-rich histone tails, consisting of up to 40 amino acid residues, protrude through the nucleosomal DNA strand, and act as a site for one of several post-translational modifications (PTMs) of chromatin (acetylation, methylation, phosphorylation, ubiquitylation, sumoylation, ADP ribosylation, deamination and proline isomerization), allowing alteration of higher order nucleosome structure.<sup>2,3</sup> There are numerous lysine methylation sites on histone tails, and PTMs at specific lysine marks can promote transcriptional activation or silencing. The flavin-dependent histone demethylase LSD1, also known as BHC110 and KDM1A,<sup>4,5</sup> catalyzes the oxidative demethylation of histone 3 methyllysine 4 (H3K4me1) and histone 3 dimethyllysine 4 (H3K4me2). Methylated histone 3 lysine 4 (H3K4) is a transcription-activating chromatin mark at gene promoters, and aberrant demethylation of this mark by LSD1 is known to silence expression of tumor suppressor genes important in human cancer.<sup>6</sup> By contrast, H3K9 methylation results in transcriptional repression.<sup>7</sup> More broadly, LSD1 is known to modulate activation or repression of a number of important genes.<sup>8</sup> Because it is overexpressed in a number of human cancers (neuroblastoma, retinoblastoma, prostate cancer, breast cancer, lung cancer, and bladder cancer),<sup>9–12</sup> LSD1 has

emerged as an important target for the development of specific inhibitors as a new class of antitumor drugs.<sup>13</sup>

To date, a handful of small molecule inhibitors of LSD1 have been described, as shown in Figure 1. Effective LSD1 inhibitors include tranylcypromine-based analogues such as 1 and 2,<sup>14,15</sup> oligoamines such as verlindamycin 3<sup>6</sup> and related isosteric ureas and thioureas,<sup>16,17</sup> and peptide based LSD1 inhibitors 4 and 5.<sup>18–21</sup> Forneris et al. described a 21-mer peptide analogous to the histone 3 lysine 4 substrate region of LSD1, wherein Lys4 was replaced by a methionine (compound 6, Figure 1).<sup>22</sup> This linear peptide was a potent inhibitor of recombinant LSD1 with a  $K_i$  value of 0.04  $\mu$ M, and inhibited LSD1 bound to CoREST with a  $K_i$  value of 0.05  $\mu$ M.<sup>22</sup> Recently, a tranylcypromine-K4H3(1–21) peptide with a  $K_i$  of 120 nM was reported.<sup>23</sup>

Cyclic peptides are generally considered to be more stable against proteolytic enzymes than their linear counterparts<sup>24</sup> and can facilitate elucidation of bioactive conformations that are important for biological activity. To date, a cyclic peptide that acts as an inhibitor of LSD1 has not been described. Peptides having less than 16 amino acid residues bind poorly to LSD1, and optimal binding appears to require 21 amino acid residues.<sup>19</sup> Thus, we used ligand-based techniques to design and synthesize a series of linear and cyclic peptides based on the 21 amino acid H3K4 binding region. Because it is a potent

**Received:** August 1, 2013

**Accepted:** November 8, 2013

**Published:** November 8, 2013

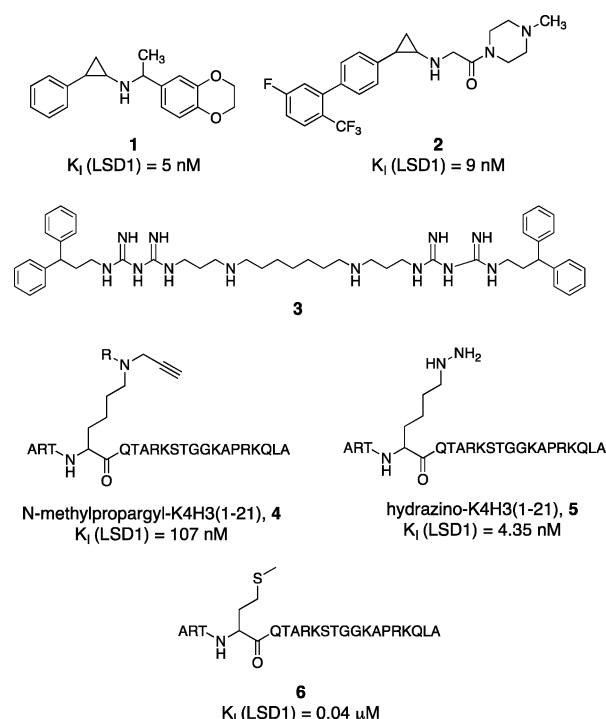


**Figure 1.** Structure of the LSD1 inhibitors **1** and **2** (tranylcypromine-based), verlindamycin **3** (oligoamine-based), and **4–6** (peptide based).

peptide-based inhibitor of LSD1, the X-ray crystallographic structure of LSD1-CoREST bound to **6** was used as the basis for the design of these cyclic peptide inhibitors. The X-ray crystallographic conformation of the bound [Met]<sup>4</sup> H3 (1–21)–OH peptide **6** revealed that the side chains of certain amino acid residues are in proximity to each other in three dimensions. For example, Arg2 and Gln5, Arg2 and Ser10, Arg2 and Gly12, Arg2 and Lys14, and Gln5 and Ser10 were identified as pairs of amino acid residues situated in close proximity (Figure 2) during LSD1 binding to **6**.

To produce peptides that were constrained in the bound conformation of **6**, we constructed peptides substituted in select positions with one Lys residue and one Glu residue, and cyclized these residues to form a lactam bridge (Table 1). Standard N-Fmoc/*tert*-Bu chemistry was used to construct all linear and cyclic peptide analogues in this study (See the Supporting Information for a complete description of the chemical synthesis). Polystyrene resin with low substitution (0.36 mmol/g) was used as a polymer support to yield all peptides as C-terminal carboxyamides.

Where appropriate, N-Fmoc amino acids not used for the lactam bridge formation were side-chain protected with acid labile protecting groups (e.g., *tert*-Bu, Boc, Trt, and Pbf), whereas Lys and Glu residues used for lactam bridge formation were side-chain protected using the orthogonal protecting groups alloc and allyl, respectively. The alloc and allyl protecting groups were selectively removed using Pd(PPh<sub>3</sub>)<sub>3</sub> in the presence of the allyl scavenger DMBA. After removing the orthogonal protecting groups, and while the peptide chain was still attached to the resin, the lactam-bridge between the side chains of Lys and Glu was formed using the coupling reagent PyBOP. The protected cyclic or linear peptide was cleaved from the solid support using TFA and an appropriate scavenger. All target peptides were purified by column

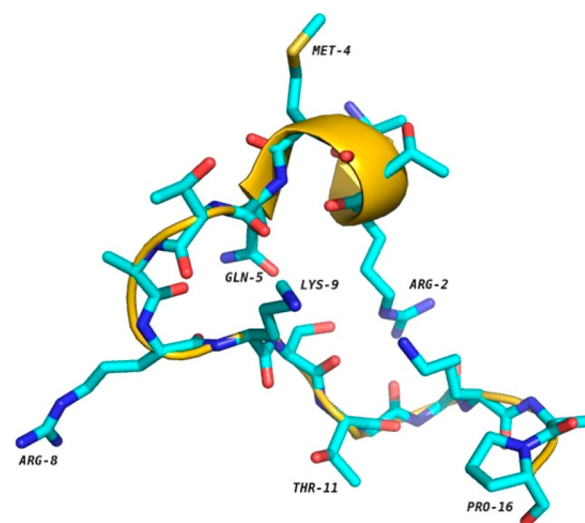


**Figure 2.** X-ray crystallographic conformation reported for **6** bound to LSD1. The primary sequence of **6** is ARTMQTARKSTGGKAPRKQLA.<sup>21</sup> Residues 1–16, which have well-defined secondary structure, are shown; residues 17–21 occur as random coils and are not shown.

**Table 1.** Percent Inhibition of LSD1 by **3**, Linear Peptide Analogues **6** and **7**, and Cyclic Peptide Analogues **8–13** at 10  $\mu$ M<sup>a</sup>

	Structure	% LSD1 Inhibited (10 $\mu$ M)
<b>6</b> <sup>22</sup>	[Met] <sup>4</sup> H3 (1-21)-OH (H-AR <sup>2</sup> TMQ <sup>5</sup> TARK <sup>9</sup> S <sup>10</sup> TGGK <sup>14</sup> APRKQLA-OH)	97 $\pm$ 2.5
<b>7</b>	[Met] <sup>4</sup> H3 (1-21)-NH <sub>2</sub> (H-AR <sup>2</sup> TMQ <sup>5</sup> TARK <sup>9</sup> S <sup>10</sup> TGGK <sup>14</sup> APRKQLA-NH <sub>2</sub> )	91 $\pm$ 0.1
<b>8</b>	C[Lys <sup>2</sup> , Glu <sup>14</sup> ] [Met] <sup>4</sup> H3 (1-21)-NH <sub>2</sub> -----K <sup>2</sup> -----E <sup>14</sup> -----	39 $\pm$ 3.8
<b>9</b>	C[Lys <sup>5</sup> , Glu <sup>10</sup> ] [Met] <sup>4</sup> H3 (1-21)-NH <sub>2</sub> -----K <sup>5</sup> -----E <sup>10</sup> -----	94 $\pm$ 0.3
<b>10</b>	C[Lys <sup>2</sup> , Glu <sup>10</sup> ] [Met] <sup>4</sup> H3 (1-21)-NH <sub>2</sub> -----K <sup>2</sup> -----E <sup>10</sup> -----	48 $\pm$ 19
<b>11</b>	C[Lys <sup>2</sup> , Glu <sup>12</sup> ] [Met] <sup>4</sup> H3 (1-21)-NH <sub>2</sub> -----K <sup>2</sup> -----E <sup>12</sup> -----	49 $\pm$ 0.6
<b>12</b>	C[Lys <sup>2</sup> , Glu <sup>5</sup> ] [Met] <sup>4</sup> H3 (1-21)-NH <sub>2</sub> -----K <sup>2</sup> -----E <sup>5</sup> -----	43 $\pm$ 12
<b>13</b>	C[Lys <sup>9</sup> , Glu <sup>14</sup> ] [Met] <sup>4</sup> H3 (1-21)-NH <sub>2</sub> -----K <sup>9</sup> -----E <sup>14</sup> -----	78 $\pm$ 0.4
<b>3</b>		95 $\pm$ 0.1

<sup>a</sup>Each data point is the average of 3 determinations that in each case varied by 5% or less. A "C" in the sequence denotes cyclic peptide.

chromatography on a CombiFlash purification system equipped with a C18 column. They were then fully characterized by UPLC, LC-MS, and high-resolution MALDI spectrometry (Table S1, Supporting Information).

The level of LSD1 inhibition for all cyclic and linear peptides was evaluated using a previously described peroxide coupled assay<sup>25,26</sup> in the presence of a fixed concentration of peptide substrate containing a dimethylated lysine residue (see Supporting Information and Table S2 for a complete protocol). Each compound was initially evaluated at a 10  $\mu$ M concentration, and an  $IC_{50}$  value was determined for the most active peptide analogue **9** over a concentration range of 0.01–50  $\mu$ M. The known LSD1 inhibitor verlindamycin **3**<sup>6</sup> was used as a positive control and produced 95% inhibition of the enzyme at 10  $\mu$ M. This level of inhibition is consistent with previously published values.<sup>27,28</sup> As shown in Table 1, all cyclic peptides inhibited the enzyme between 39 and 94%, following the relative rank order of **9** > **7** > **13** > **11** = **10** > **12** > **8**. Thus, the [Met]<sup>4</sup> H3 (1–21)-NH<sub>2</sub> cyclic peptide **9**, in which the lactam bridge was between Lys5 and Glu10, produced the greatest LSD1 inhibitory activity, while cyclic [Lys2, Glu14] [Met]<sup>4</sup> H3 (1–21)-NH<sub>2</sub> **8** displayed the least inhibitory activity. The reduced potency of **8** and **10**–**12** could in part be due to the replacement of arginine at the 2 position, which is known to have a critical interaction with the enzyme.<sup>22</sup> As shown in Figure 3, the  $IC_{50}$  value for inhibitor **9** was

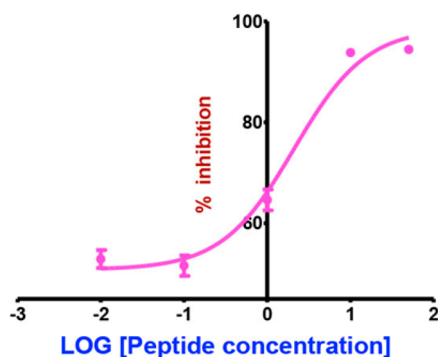


**Figure 3.** Determination of the  $IC_{50}$  value for **9** against purified recombinant LSD1. Inhibition values were gathered at concentrations between 0.01 and 50  $\mu$ M.

determined to be 2.1  $\mu$ M. Interestingly, both [Met]<sup>4</sup> H3 (1–21)-OH **6** and the corresponding carboxamide [Met]<sup>4</sup> H3 (1–21)-NH<sub>2</sub> **7**, which are identical in amino acid sequence but differ in their C-terminal functional group, were effective inhibitors, although **7** was somewhat less potent.

Inhibitors **3**, **7**, and **9** were next evaluated for their antitumor effect in the MCF-7 breast and Calu-6 lung tumor lines in vitro using an MTS cell viability assay.<sup>29,30</sup> (See Supporting Information for the MTS assay protocol and Figures S1 and S2 for results). Inhibition of MCF-7 cell proliferation was determined at concentrations between 5.0 and 300  $\mu$ M for **7** and **9** and between 0.4 and 200  $\mu$ M for **3**. Similarly, inhibition of Calu-6 cell proliferation was determined at concentrations between 1 and 200  $\mu$ M for **7** and **9** and between 0.76 and 200  $\mu$ M for **3**. At 72 h, inhibitors **7** and **9** displayed calculated  $IC_{50}$  values of 152.6 and 156.6  $\mu$ M, respectively, in MCF-7 cells and 120.7 and 125.3  $\mu$ M in Calu-6 cells, compared to  $IC_{50}$  values of 5.9 and 10.9  $\mu$ M for **3** in MCF-7 and Calu-6 cells, respectively. The relatively low antitumor potency following treatment with

**7** and **9** as compared to **3** could be due to reduced transport into the cell nucleus, and additional experiments are underway to verify this hypothesis. In any case, cell penetration can be enhanced through modification of the cyclic peptide structure.

To assess the in vitro metabolic stability of linear peptide **7** and cyclic peptide **9**, the half-lives for their hydrolytic degradation were determined by incubating them in rat plasma at 25 °C (see Supporting Information for a complete protocol).<sup>31</sup> As shown in Figure 4, cyclic peptide **9** was significantly more stable ( $T_{1/2}$  = 59.8 min) compared to the linear peptide **7** ( $T_{1/2}$  = 14.3 min).

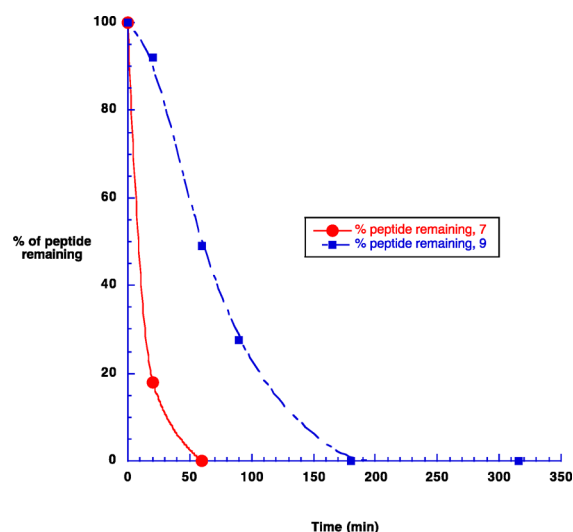


**Figure 4.** Metabolic stability of linear peptide **7** and cyclic peptide **9** in rat plasma. See Supporting Information for the metabolic degradation protocol.

It has been reported that the demethylated natural 21 amino acid H3K4 peptide competitively inhibits LSD1 with a  $K_i$  of 1.8  $\mu$ M.<sup>7</sup> The cyclic peptide **9** also proved to be a competitive inhibitor of the enzyme with a  $K_i$  of 385 nM (see Supporting Information for a complete protocol, and Figures S3–S9 and Tables S3 and S4 for results). To determine the inhibition constant ( $K_i$ ) and elucidate the mechanism of LSD1 inhibition, initial rates were evaluated using a peroxide coupled assay with varying final substrate concentrations between 0 and 100  $\mu$ M and final concentrations of **9** between 0 and 1  $\mu$ M (Figures S3–S6, Supporting Information). The substrate velocity data for varying concentrations of **9** was then subjected to Michaelis–Menten analysis (Figures S7–S9 and Tables S3 and S4, Supporting Information) and revealed a  $V_{max}$  of 54.4  $\mu$ mol/min/mg of protein and a  $K_m$  of 15.3  $\mu$ M, respectively. A Lineweaver–Burke plot (Figure S8, Supporting Information) confirmed **9** was a competitive inhibitor of LSD1. Finally, the substrate velocity data was fitted for the competitive type inhibition using GraphPad Prism 5 software (GraphPad, San Diego, California);  $K_i$ ,  $K_m$ , and  $V_{max}$  values were 385 nM, 14.46  $\mu$ M, and 14.46  $\mu$ M/min/mg protein (Figure S9 and Table S4, Supporting Information).

In order to understand the inhibitory activity of **9**, it was compared in silico to the reported X-ray crystallographic conformation of **6**. The global least energy conformation of **9** was obtained using the Monte Carlo MacroModel (MCM) search algorithm.<sup>32,33</sup> As shown in Figure 5, the least energy conformation of **9** features a right-handed alpha helical section



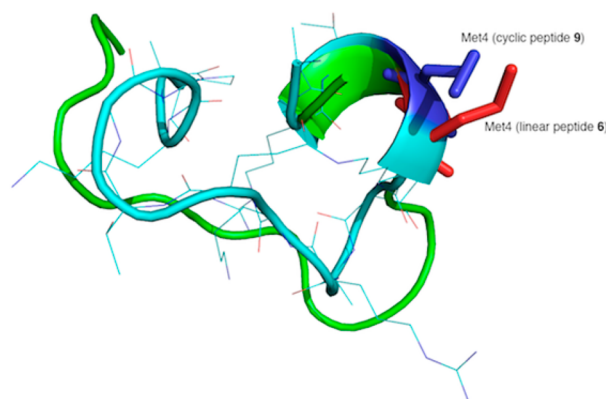


**Figure 5.** Structural superimposition of linear peptide 6 and cyclic peptide 9. Amino acids 1–16 are shown for both peptides. The green color represents the X-ray crystallographic conformation of 6 as reported in PDB file 2V1D. The cyan color represents the global least energy conformation of 9 derived from the MCMM algorithm of MacroModel. Met4 of 6 and 9 are shown in red and blue, respectively.

and a  $\beta$  sheet section. When the MCMM-derived conformation of amino acid residues 1–16 of 9 was compared with that of 6, the compounds were found to assume very similar backbone and local side chain conformations. This similarity in least energy conformations of the 9 and 6 could explain their similar ability to inhibit recombinant LSD1.

The 50 lowest energy conformations obtained from MCMM analysis were compared by examination of their backbone dihedral angles  $\phi$  and  $\psi$  in a Ramachandran plot (Figure S10 and S11, Supporting Information). All of the amino acids except Gly12 and Gly13 display a very narrow range of distribution of dihedral angles. This confirms that there can be a rigid conformation in all amino acids except Gly12 and Gly13. Two groups of amino acid residues, one containing Arg8, Lys9, Glu10 and Ala15 and the other containing Arg2, Thr3, Met4, Lys5, Lys14 fall in the regions of the  $\beta$  sheet and right handed  $\alpha$  helix in Ramachandran plot, respectively (Figures S11–S12 and Table S5, Supporting Information). Interestingly, the dihedral angle for the Gly12 promotes a right-handed  $\alpha$  helix or a  $\beta$  sheet, whereas Gly12 promotes a right-handed  $\alpha$  helix or a left-handed  $\alpha$  helix. Moreover, Thr6 falls into an energetically unfavorable region of the Ramachandran plot. It appears that Thr6 adopts a strained conformation due to the local constraint introduced by cyclization.

In conclusion, we developed a novel cyclic peptide 9 that exhibits potent LSD1 inhibition in vitro. The structures obtained from the conformational analysis and their dihedral angle distributions provide novel insight into the bioactive conformations of 9 as it pertains to LSD1 inhibition. Further, presumably due to the cyclic nature of the peptide, 9 displays enhanced stability against proteolytic degradation and has moderate antitumor effects in vitro in 2 tumor cell lines. The discovery of additional, more effective cyclic peptides related to 9 is an ongoing concern in our laboratories.

## ■ ASSOCIATED CONTENT

### ■ Supporting Information

Chemical synthesis; characterization of target peptides; enzyme inhibition procedures; stability procedures, cell culture protocols, and conformational analysis; and statistical analysis. This material is available free of charge via the Internet at <http://pubs.acs.org>.

## ■ AUTHOR INFORMATION

### Corresponding Author

\*(P.M.W.) E-mail: [woster@musc.edu](mailto:woster@musc.edu).

### Author Contributions

All authors have given approval to the final version of the manuscript

### Funding

The research described in this letter was supported by NIH/NCI award RO1-CA149095 (to P.M.W.).

### Notes

The authors declare no competing financial interest.

## ■ ABBREVIATIONS

LSD1, lysine-specific demethylase 1; H3K4, histone 3 lysine 4; H3K4me, histone 3 methyllysine 4; H3K4me, two histone 3 dimethyllysine 4; CoREST, RE1-silencing transcription factor corepressor 1; DMBA, 1,3-dimethylbarbituric acid; MCMM, Monte Carlo Multiple minimum

## ■ REFERENCES

- (1) Strahl, B. D.; Allis, C. D. The language of covalent histone modifications. *Nature* **2000**, *403* (6765), 41–45.
- (2) Jenuwein, T.; Allis, C. D. Translating the histone code. *Science* **2001**, *293* (5532), 1074–1080.
- (3) Latham, J. A.; Dent, S. Y. Cross-regulation of histone modifications. *Nat. Struct. Mol. Biol.* **2007**, *14* (11), 1017–1024.
- (4) Shi, Y. Histone lysine demethylases: emerging roles in development, physiology and disease. *Nat. Rev. Genet.* **2007**, *8* (11), 829–833.
- (5) Shi, Y.; Lan, F.; Matson, C.; Mulligan, P.; Whetstone, J. R.; Cole, P. A.; Casero, R. A.; Shi, Y. Histone demethylation mediated by the nuclear amine oxidase homolog LSD1. *Cell* **2004**, *119* (7), 941–953.
- (6) Huang, Y.; Greene, E.; Stewart, T. M.; Goodwin, A. C.; Baylin, S. B.; Woster, P. M.; Casero, R. A. Inhibition of lysine-specific demethylase 1 by polyamine analogues results in reexpression of aberrantly silenced genes. *Proc. Natl. Acad. Sci. U.S.A.* **2007**, *104*, 8023–8028.
- (7) Forneris, F.; Binda, C.; Vanoni, M. A.; Battaglioli, E.; Mattevi, A. Human histone demethylase LSD1 reads the histone code. *J. Biol. Chem.* **2005**, *280* (50), 41360–41365.
- (8) Suzuki, T.; Miyata, N. Lysine demethylases inhibitors. *J. Med. Chem.* **2011**, *54* (24), 8236–8250.
- (9) Hayami, S.; Kelly, J. D.; Cho, H. S.; Yoshimatsu, M.; Unoki, M.; Tsunoda, T.; Field, H. I.; Neal, D. E.; Yamaue, H.; Ponder, B. A.; Nakamura, Y.; Hamamoto, R. Overexpression of LSD1 contributes to human carcinogenesis through chromatin regulation in various cancers. *Int. J. Cancer* **2011**, *128* (3), 574–586.
- (10) Lim, S.; Janzer, A.; Becker, A.; Zimmer, A.; Schule, R.; Buettner, R.; Kirfel, J. Lysine-specific demethylase 1 (LSD1) is highly expressed in ER-negative breast cancers and a biomarker predicting aggressive biology. *Carcinogenesis* **2010**, *31* (3), 512–520.
- (11) Schulte, J. H.; Lim, S.; Schramm, A.; Friedrichs, N.; Koster, J.; Versteeg, R.; Ora, I.; Pajtl, K.; Klein-Hitpass, L.; Kuhfittig-Kulle, S.; Metzger, E.; Schule, R.; Eggert, A.; Buettner, R.; Kirfel, J. Lysine-specific demethylase 1 is strongly expressed in poorly differentiated neuroblastoma: implications for therapy. *Cancer Res.* **2009**, *69* (5), 2065–2071.
- (12) Rotili, D.; Mai, A. Targeting histone demethylases: A new avenue for the fight against cancer. *Genes Cancer* **2011**, *2* (6), 663–679.
- (13) Stavropoulos, P.; Hoelz, A. Lysine-specific demethylase 1 as a potential therapeutic target. *Expert Opin. Ther. Targets* **2007**, *11* (6), 809–820.
- (14) Guibourt, N.; Ortega-Munoz, A.; Castro-Palomino Laria, J. Preparation of phenylcyclopropylamine derivatives as LSD1 selective

and LSD1/MAO-B dual inhibitors in treating or preventing cancer. PCT WO 2010084160, 2010.

(15) Ortega-Munoz, A.; Castro-Palomino Laria, J.; Fyfe, M. C. T. Lysine-specific demethylase 1 inhibitors and their use. PCT application WO 2011035941 A1 20110331, 2011.

(16) Sharma, S.; Wu, Y.; Steinbergs, N.; Crowley, M.; Hanson, A.; Casero, R. A. J.; Woster, P. (Bis)urea and (bis)thiourea inhibitors of lysine-specific demethylase 1 as epigenetic modulators. *J. Med. Chem.* **2010**, *53* (14), 5197–5212.

(17) Sharma, S. K.; Hazeldine, S.; Crowley, M. L.; Hanson, A.; Beattie, R.; Varghese, S.; Sennanayake, T. M. D.; Hirata, A.; Hirata, F.; Huang, Y.; Wu, Y.; Steinbergs, N.; Murray-Stewart, T.; Bytheway, I.; Casero, R. A.; Woster, P. M. Polyamine-based small molecule epigenetic modulators. *MedChemComm* **2012**, *3*, 14–21.

(18) Culhane, J. C.; Szwczuk, L. M.; Liu, X.; Da, G.; Marmorstein, R.; Cole, P. A. A mechanism-based inactivator for histone demethylase LSD1. *J. Am. Chem. Soc.* **2006**, *128* (14), 4536–4537.

(19) Culhane, J. C.; Wang, D.; Yen, P. M.; Cole, P. A. Comparative analysis of small molecules and histone substrate analogues as LSD1 lysine demethylase inhibitors. *J. Am. Chem. Soc.* **2010**, *132* (9), 3164–3176.

(20) Szwczuk, L. M.; Culhane, J. C.; Yang, M.; Majumdar, A.; Yu, H.; Cole, P. A. Mechanistic analysis of a suicide inactivator of histone demethylase LSD1. *Biochemistry* **2007**, *46* (23), 6892–6902.

(21) Yang, M.; Culhane, J. C.; Szwczuk, L. M.; Gocke, C. B.; Brautigam, C. A.; Tomchick, D. R.; Machius, M.; Cole, P. A.; Yu, H. Structural basis of histone demethylation by LSD1 revealed by suicide inactivation. *Nat. Struct. Mol. Biol.* **2007**, *14* (6), 535–539.

(22) Forneris, F.; Binda, C.; Adamo, A.; Battaglioli, E.; Mattevi, A. Structural basis of LSD1-CoREST selectivity in histone H3 recognition. *J. Biol. Chem.* **2007**, *282* (28), 20070–20074.

(23) Ogasawara, D.; Itoh, Y.; Tsumoto, H.; Kakizawa, T.; Mino, K.; Fukuhara, K.; Nakagawa, H.; Hasegawa, M.; Sasaki, R.; Mizukami, T.; Miyata, N.; Suzuki, T. Lysine-specific demethylase 1-selective inactivators: protein-targeted drug delivery mechanism. *Angew. Chem., Int. Ed.* **2013**, *52* (33), 8620–8624.

(24) Hruby, V. J. Designing peptide receptor agonists and antagonists. *Nat. Rev. Drug Discovery* **2002**, *1* (11), 847–858.

(25) Forneris, F.; Binda, C.; Dall'Aglio, A.; Fraaije, M. W.; Battaglioli, E.; Mattevi, A. A highly specific mechanism of histone H3-K4 recognition by histone demethylase LSD1. *J. Biol. Chem.* **2006**, *281* (46), 35289–35295.

(26) Zhou, M.; Diwu, Z.; Panchuk-Voloshina, N.; Haugland, R. P. A stable nonfluorescent derivative of resorufin for the fluorometric determination of trace hydrogen peroxide: applications in detecting the activity of phagocyte NADPH oxidase and other oxidases. *Anal. Biochem.* **1997**, *253* (2), 162–168.

(27) Pachaiyappan, B.; Woster, P. M. Design of Small-Molecule Epigenetic Modulators. *Bioorg. Med. Chem. Lett.*, **2013**, DOI: dx.doi.org/10.1016/j.bmcl.2013.11.001.

(28) Hazeldine, S.; Pachaiyappan, B.; Steinbergs, N.; Nowotarski, S.; Hanson, A. S.; Casero, R. A., Jr.; Woster, P. M. Low molecular weight amidoximes that act as potent inhibitors of lysine-specific demethylase 1. *J. Med. Chem.* **2012**, *55* (17), 7378–7391.

(29) Cory, A. H.; Owen, T. C.; Barltrop, J. A.; Cory, J. G. Use of an aqueous soluble tetrazolium/formazan assay for cell growth assays in culture. *Cancer Commun.* **1991**, *3* (7), 207–212.

(30) Izumiyama, K.; Nakagawa, M.; Yonezumi, M.; Kasugai, Y.; Suzuki, R.; Suzuki, H.; Tsuzuki, S.; Hosokawa, Y.; Asaka, M.; Seto, M. Stability and subcellular localization of API2-MALT1 chimeric protein involved in t(11;18) (q21;q21) MALT lymphoma. *Oncogene* **2003**, *22* (50), 8085–8092.

(31) Yamamoto, T.; Nair, P.; Ma, S. W.; Davis, P.; Yamamura, H. I.; Vanderah, T. W.; Porreca, F.; Lai, J.; Hruby, V. J. The biological activity and metabolic stability of peptidic bifunctional compounds that are opioid receptor agonists and neurokinin-1 receptor antagonists with a cystine moiety. *Bioorg. Med. Chem.* **2009**, *17* (20), 7337–7343.

(32) Chang, G.; Guida, W. C.; Still, W. C. An internal-coordinate Monte Carlo method for searching conformational space. *J. Am. Chem. Soc.* **1989**, *111* (12), 4379–4386.

(33) Saunders, M.; Houk, K. N.; Wu, Y.-D.; Still, W. C. Conformations of cycloheptadecane: A comparison of methods for conformational searching. *J. Am. Chem. Soc.* **1990**, *112*, 1419–1427.